LA-UR- 98-2424

Approved for public release;
distribution is unlimited.

Title: EXTERNAL Q STUDIES FOR APT SUPERCONDUCTING CAVITY COUPLERS

CONF-980827--

Author(s): Pascal Balleyguier

Submitted to: LINAC 98 Conference
Chicago, IL
August 24-28, 1998

Los Alamos
NATIONAL LABORATORY

DISCLAIMER

External Q Studies for APT Superconducting Cavity Couplers*

Pascal Balleyguier

Abstract
Coupling coefficients for the APT superconducting cavity couplers have been predicted using an improvement of the method previously developed for the French Trispal project [1]. We here present the method and a proof of the formula used to compute the external Q. Measurements on a single-cell copper cold model exhibited a very good agreement against simulation. Then, we established that the original coupler design lead to an insufficient coupling in β=0.64 cavities. Different solutions were proposed to fix this problem, like combining impedance discontinuities in the line and an off-centered disc end tip. Finally, it was decided to increase the beam tube diameter though it has some influence on the cavity end-cell performance.

*Work supported by the US Department of Energy

1. Introduction

The superconducting accelerating cavity prototype for the Accelerator Production of Tritium project and its associated power coupler have been intensively studied in Los Alamos [2]. Among the main characteristics is the external quality factor of the cavity. This parameter determines the coupling between the cavity and the RF line that feeds it.

Some methods to compute the external Q already exist. In 1990, Kroll and Yu [3] proposed one based on a fit on a branch of the Slater's diagram (fig.1). Unfortunately, this method is limited to low Qext values (less than a few hundreds) and is not suitable for our purpose. The author of the present paper recently proposed a new method [4]. It has been improved since, and the resulting method in fact is equivalent in its principle to another one described in 1993 by Hartung and Haebel [5]. However, our method differs both in the proof and in the practical way to operate. Moreover, we derive from it a procedure to compute fields and local power losses under operation in a cavity and its power coupler.

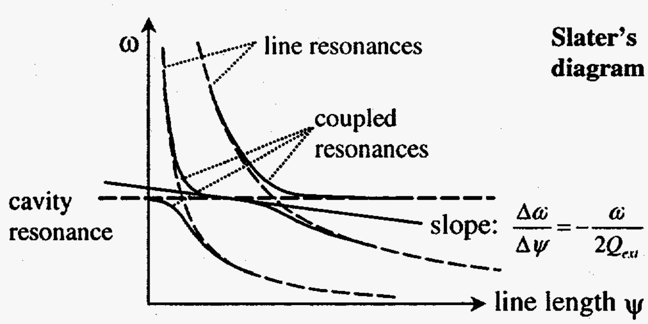

Fig. 1. Slater's diagram and Kroll-Yu's formula.

2. Method

2.1 Travelling waves

Let us consider a lossless cavity initially containing some RF energy W at its resonant frequency ω. If this cavity is weakly coupled to an infinite line, this line drives out a certain RF power P and the energy stored in the cavity gradually decreases. The external Q then is:

$$Q_{ext} = \frac{\omega W}{P}$$

Only a single mode is assumed to travel along the line. The power transported by the travelling wave along the line may be computed either from the electric or the magnetic field amplitude:

$$P = \frac{1}{2\eta}\iint_{\text{line x sect}} |E|^2 ds = \frac{\eta}{2}\iint_{\text{line x sect}} |H|^2 ds,$$

assuming that η is the mode impedance. The stored energy in the cavity (assumed to be under vacuum) is:

$$W = \frac{1}{2}\iiint_{cavity} \varepsilon_0 |E|^2 dv = \frac{1}{2}\iiint_{cavity} \mu_0 |H|^2 dv.$$

We assume the line mode is a TEM, and that the dielectric is vacuum: $\eta^2=\mu_0/\varepsilon_0$. Then, the external Q can be expressed as:

$$Q_{ext} = \frac{\omega \iiint_{cavity} |F|^2 dv}{c\iint_{\text{line x sect}} |F|^2 ds}, \qquad (1)$$

F being either the electric (*E*) or magnetic (*H*) field. (If the line is not under vacuum and/or the mode is not a TEM one, a coefficient taking the line mode impedance into account has to be introduced in equation (1)).

Unfortunately, computing the Qext with the formula (1) would require the use of a dissipative code. Though such codes now exist, they are more difficult to use and much slower than non-dissipative ones.

2.2 Standing waves

Inverting the sign of time gives a second solution of Maxwell's equations that represents the same cavity slowly gaining energy from an incoming wave travelling in the line. According to the superposition theorem, we can add these two solutions (fig. 2).

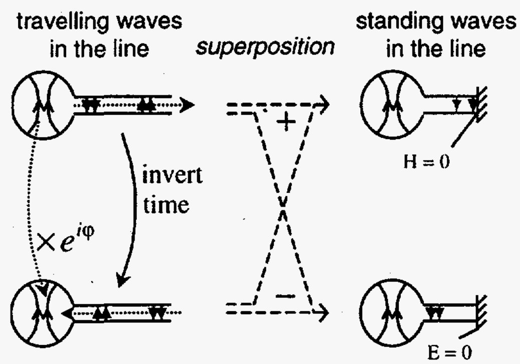

Fig. 2. Transforming a travelling-wave problem into a standing-wave one.

Inside the line, the two added travelling waves drive the same RF power P in either direction, and they interfere into a standing wave. Let us choose the reference plane at an electric field antinode: the standing wave field amplitude is there twice the one of the travelling waves. Inside the cavity, the two added fields have an arbitrary phase difference φ, so the amplitude of the resulting field is $|1+e^{i\varphi}|$ times the one of the original field. Using the same formal expression as in equation (1), we can define the quantity Q_1 as:

$$Q_1 = \frac{\omega \iiint_{cavity} |E_1|^2 dv}{c \iint_{ref..plane} |E_1|^2 ds} = \frac{|1+e^{i\varphi}|^2}{4} Q_{ext},$$

where the suffix *1* indicates the resulting field after addition. This field is a pure standing wave in both the cavity and the line. The line can be terminated at the reference plane with the appropriate boundary condition (perfect magnetic wall) without changing the fields, making this problem computable by MAFIA.

Now let us use the superposition theorem again, but by subtracting the two solutions instead of adding them (the resulting fields will be noted with the suffix 2). At the same reference plane, we now have a magnetic antinode which field amplitude is twice the one of the travelling wave. Inside the cavity, the resulting field is now $|1-e^{i\varphi}|$ times the original field. We define Q_2 as:

$$Q_2 = \frac{\omega \iiint_{cavity} |H_2|^2 dv}{c \iint_{ref..plane} |H_2|^2 ds} = \frac{|1-e^{i\varphi}|^2}{4} Q_{ext}.$$

This problem can also be computed by MAFIA with the other boundary condition (perfect electric wall) at the reference plane. As for any value of φ, $|1+e^{i\varphi}|^2 + |1-e^{i\varphi}|^2 = 4$, we have then:

$$Q_{ext} = Q_1 + Q_2.$$

So, two MAFIA runs (with the same mesh) are sufficient to predict the external Q. The reference plane can be chosen anywhere in the line: its position should not have any influence on the external Q, provided that only one mode can propagate up to the reference plane.

2.3 Line length independence

As an example, fig. 3 is a plot of the external Q computed for the APT β=0.82 superconducting cavity. Various line lengths have been taken: they all give the same final result within less than 0.5% variations. This result has been obtained with double precision computations because single precision lead to 10 % fluctuations.

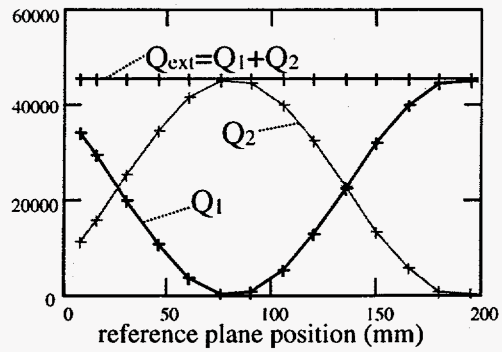

Fig. 3. Influence of the line length in Q_{ext} computations.

2.4 Reconstitution of the travelling wave.

Reciprocally, the travelling wave can be reconstituted from the two standing wave solutions in order to compute the fields in normal operation. For this purpose, one just has to combine the two standing waves solutions in quadrature phase (fig. 4). Before combining, one has to make sure that the electromagnetic energy at an arbitrary line cross section of the line is the same for the two waves to combine.

This operation also permits to compute the losses in the coupler under normal operation. As the two solutions to be combined are in quadrature phase, the losses of the combination are just the sum of the losses of the two solutions, after normalizing them with respect to the energy density at the line end plane.

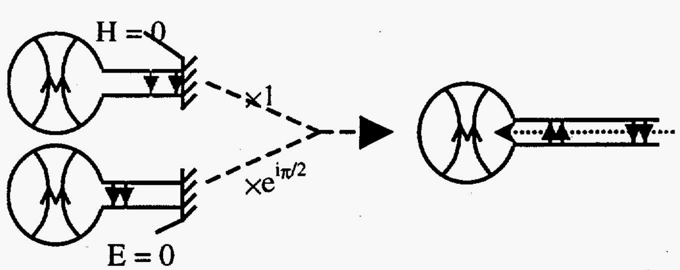

Fig. 4. Reconstitution of the travelling wave.

3. Experimental validation

To prove the validity of this method, we used it on the β=0.64 single-cell copper mock-up cavity. The coupling can be changed by moving the electrical antenna more or less into the beam tube. Experimentally, external Q's have been measured by two methods: reflection and transmission (fig.5).

In the reflection method we measure the VSWR with an s_{11}-calibrated network analyzer, and deduce the coupling coefficient β: β=1/VSWR if the cavity is under-coupled (i.e. the polar plot of the reflection coefficient does not circle the origin), and β=VSWR in case of over coupling. The loaded Q is given by the inverse of the relative 3-dB bandwidth measured with an auxiliary low-coupled antenna. This second antenna has not to be calibrated. Both internal and external Q's can be deduced from this measurement with the following formulas:

$$Q_{ext} = \left(1+\beta^{-1}\right)Q_{load}, \quad \text{and} \qquad Q_{\text{int}} = \left(1+\beta\right)Q_{load}.$$

The last equation should give a constant value even in case of coupling variations, and it is a good check for the quality of the measurements.

The transmission method requires a preliminary calibration of an auxiliary antenna in reflection by the method described above. The auxiliary antenna external Q will be noted Q_{aux}. Then the network analyzer should be calibrated in transmission (s_{21}). Then, the 1 and 2 ports of the network analyzer are connected to the auxiliary antenna, and the to coupler output respectively. The coupler external Q is the given by:

$$Q_{ext} = \frac{1}{Q_{aux}}\left(\frac{2Q_{load}}{\tau}\right)^2,$$

in which τ is the voltage transmission coefficient deduced from the measured s_{21} attenuation *a* in dB:

$$\tau = 10^{-\frac{a}{20}}.$$

Practically, it is interesting to position the auxiliary antenna for a β=1 coupling. In this case, the auxiliary antenna external Q equals the internal Q. If the coupler external Q to measure is much higher (case of low coupling), its influence on the loaded Q can be neglected, and we have:

$$Q_{load} = \frac{Q_{\text{int}}}{2} = \frac{Q_{aux}}{2} << Q_{ext},$$

leading to:

$$Q_{ext} \approx \frac{1}{\tau^2}.$$

The Q_{ext} has been computed and measured for various penetrations of the coupler antenna. Results plotted on figure 6 show an excellent agreement between the simulation and the measurements. The discrepancy is less than 20 % for reflection measurements and less 7 % for transmission measurements.

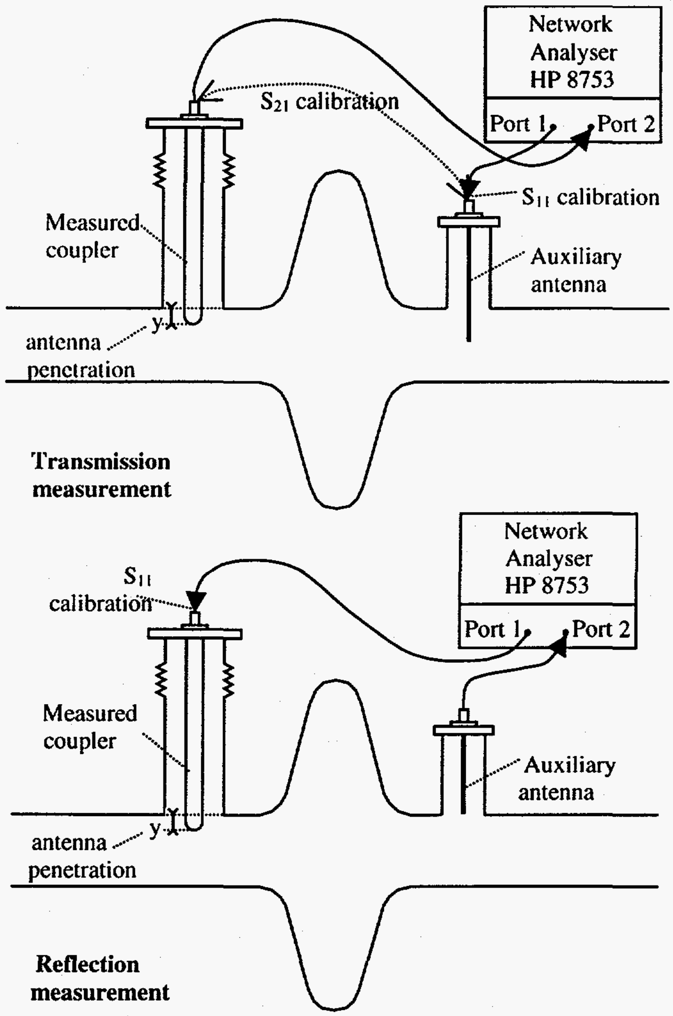

Fig. 5. Q_{ext} measurement by reflection and transmission in the mock-up cavity

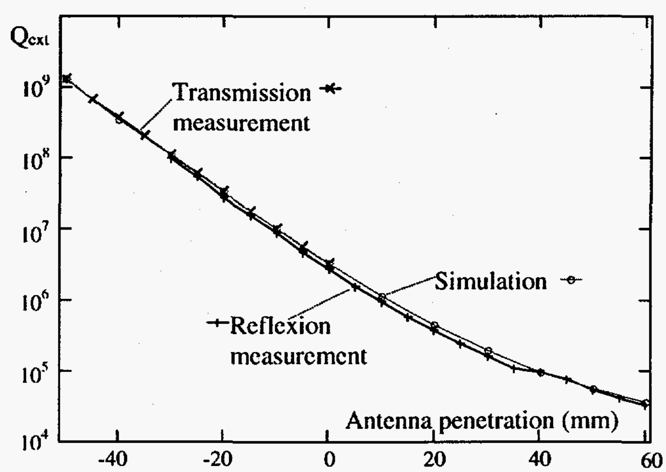

Fig. 6. External Q computation and measurement in the 1-cell β=0.64 copper mock-up cavity.

4. The β=0.64 APT cavity

4.1 Required external Q

The external Q must equal the internal Q (actually the beam Q, because RF losses are negligible in a superconducting cavity), in order to avoid reflected power under normal operation. The internal Q is:

$$Q_{int} = \frac{\omega W}{P_{beam}},$$

where W is the stored energy, and P_{beam} the power gained by the beam. It can be written as:

$$Q_{int} = \frac{\omega W}{UI\cos\varphi},$$

where U is the accelerating voltage seen by a synchronous particle, and φ is the phase angle between the proton bunch and the RF voltage. Considering a single cell, the accelerating voltage is linked to the gradient E by:

$$U = \beta \lambda/2 E.$$

The energy stored in the single cell is linked to its geometrical impedance (circuit definition) by:

$$r/Q = \frac{U^2}{2\omega W}.$$

Combining the last three equations leads to:

$$Q_{int} = \frac{\beta \lambda/2 E}{2\, r/Q\, I\cos\varphi}.$$

The geometric impedance of a single cell had been previously computed with MAFIA: r/Q= 17.1 Ω. With β=0.64, E=4.8 MV/m, I=100mA (beam current), φ=30°, we get:

$$Q_{int}=0.222\times10^6,$$

which is the goal value for Qext.

4.2 Coupler original design.

The cavity (desrcibed in [6]) has been simulated with the originally designed power coupler (fig.7): a 50 Ω coaxial line, the inner conductor (22-mm radius) being ended by a hemisphere that is flush with the beam tube (penetration = 0). According to the plans, the outer conductor is 25.4 mm away from the end of the last cell. Only a quarter of a single cell has been computed. With the 3 symmetries used, this represents a 2-cell cavity equipped with four couplers.

The raw results were Q_1=192000 and Q_2= 106000. For a 5-cell cavity with only two couplers, the stored energy is 5/2 larger, but the total power traveling through the couplers is reduced by a factor 2/4. So, in a real cavity, we anticipated that:

$$Q_{ext} = (Q_1 + Q_2)\frac{5/2}{2/4} = 1.49\times10^6.$$

The conclusion is that the Qext is off by a factor 1.49/0.222=6.7. Expressed with a log scale, the coupling has to be increased by: -10×log(0.22/1.46)=+8.3 dB. As shown on figure 8, with such a design, the antenna needs to be pushed 26 mm into the beam pipe in order to reach the goal: this is not acceptable in a real accelerator. The next section describes a first attempt to fix this problem without any modification to the cavity.

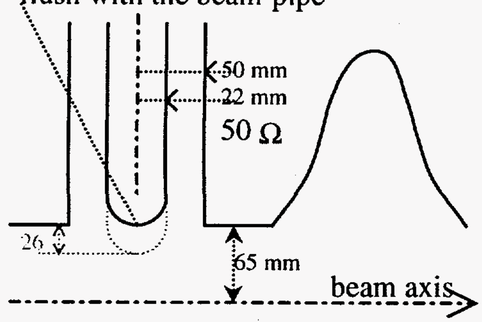

Qext=1.5×10^6 (–8.3 dB from goal)

Fig. 7. Original coupler design (β.64)

Qext vs antenna penetration

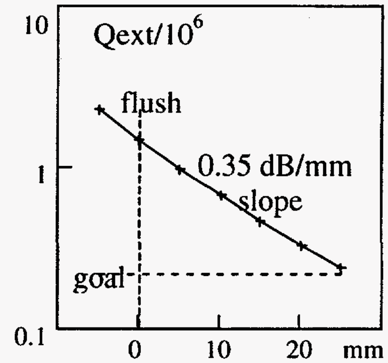

Fig. 8. Influence of antenna penetration (original design).

5. Solution without cavity modification

5.1 End tip modifications

Replacing the hemisphere with a flat end, with the same antenna length, increases the coupling factor. Qext=0.985×10^6, i.e. an improvement of 1.8 dB (Fig. 9a). Simulations showed that enlarging the antenna end tip with an axial disc has only a minor influence on the coupling. However, an off-centered disc directed toward the accelerating cells does have an important effect. With a 10 mm thickness, and a 14 mm gap between the disc and the coupler tube (Fig 9b), one gets: Qext=0.51×10^6, which is 2.9 dB better than the flat end tip, but still too high compared to the goal.

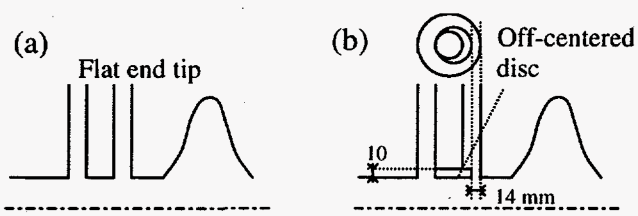

Qext=1.0×10^6 (-6.5 dB from goal)   Qext=0.51×10^6 (-3.6 dB from goal)

Fig. 9. (a):Flat end tip. (b):With off-centered disc.

5.2 Impedance step.

As seen on figure 10, changing the line impedance with a constant outer line diameter does not significantly improve the coupling. However, a way to increase the coupling (suggested by Henri Safa) is to make an impedance discontinuity in the coaxial line. This discontinuity generates a reflection that can be combined with the one at the antenna end. If the distance between those two reflections is suitably chosen, the two reflected waves partially cancel each other, and the matching is improved.

In a first approximation, the antenna end can be seen as an open circuit. An increase of the line outer radius λ/2 away from the antenna end (which increases the impedance) generates a standing wave between those two planes. Keeping the internal diameter of the line constant as the outer diameter changes permits to generate this impedance discontinuity. As the outgoing line has to have a 50 Ω impedance, this leads to a 25-Ω line impedance at the end of the line (cavity side). After optimizing the distance between the impedance change and the end tip, we reached: Qext=0.49×10^6 (fig.11). The coupling gain is +3 dB with respect to a simple flat-ended antenna of constant impedance and 50-mm outer conductor radius.

The resonant coupler effect can be enforced by a second discontinuity: the internal radius can vary too in order to keep the original 22-mm radius at the antenna end. As this impedance step is in the opposite sense, it has to be placed λ/4 further into the line to make a positive effect. With such a geometry (fig. 12) we obtained: Qext=0.45×10^6, i.e. + 3.4 dB compared to original coupler with a flat end tip.

It is not much better than the single step coupler, but the main advantage of the last solution is that the end tip is similar to the original one. So, we can add an off-centered disc to increase the coupling. With a slightly smaller disc (gap=17 mm) and a smaller conductor (17-mm radius) we finally obtained the needed coupling (fig. 13).

However, the above solution only barely gave the necessary Qext and would have let no margin in case of unexpected behavior. For this reason, the solution described in the next section was preferred.

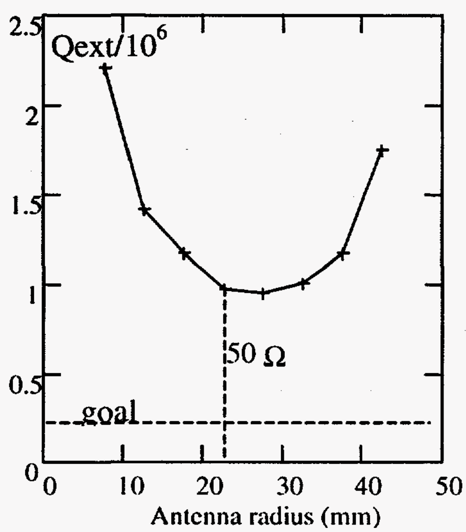

Fig. 10. Influence on antenna radius

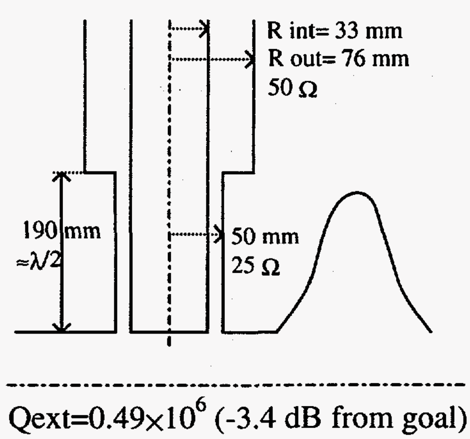

Fig. 11. Resonant coupler with a 25 Ω final impedance.

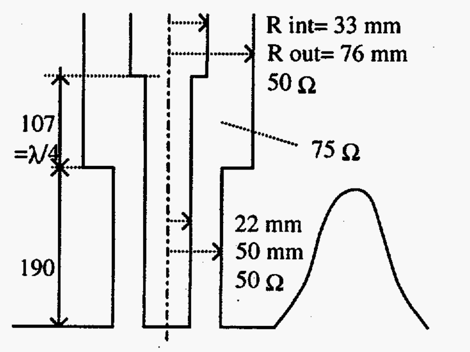

Qext=0.45×10^{6} (-3.1 dB from goal)

Fig. 12. Resonant coupler with a double impedance discontinuity.

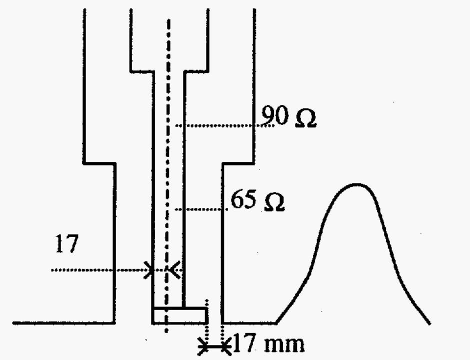

Qext=0.22×10^{6}: goal achieved

Fig. 13. Double impedance discontinuity combined with asymmetric end tip.

6. Beam tube expansion.

Modifying the cavity itself could also improve the coupling. For technical reason, it was impossible to reduce the distance between the coupler and the end-cell. But expanding the end-cell beam-pipe radius from 65 to 80 mm was rather easy, as 80 mm is already the beam pipe radius of the β=0.82 cavities.

6.1 Corrections

Such a modification in the cavity geometry has of course some influence on its performance. First of all, the end cell profile has to be adjusted in order to keep a 700 MHz resonance frequency. This was done by reducing the major ellipse diameter from 120 to 97 mm. As a result, the transit time factor is poorer in the enlarged tube end cell, and the geometric impedance (r/Q) drops by 19 %. So the r/Q per cell (averaged over the whole cavity) is 96.3% of the original design one, i.e. 16.5 Ω instead of 17.1 Ω (circuit definition). This changes the beam Q (and the required Qext) from 0.222×10^{6} to 0.230×10^{6}. We assume here that the average accelerating gradient remains equal to 4.8 MV/m. Moreover, as the enlarged tube end cavity holds a little more of energy than the four other ones (20.77% of the 5-cell cavity), the extrapolation factor (from 2-cell 4-coupler to 5-cell 2-coupler) should be 4.815 instead of 5.

6.2 Final design

Computations showed that enlarging the beam tube would dramatically increase the coupling: the Qext value (0.255×10^{6}) was almost the required one. In order to further improve the coupling, a 10-mm thick symmetrical disc was added at the antenna end tip. On figure 14, the disc radius was varied from 22 to 34 mm: the extra radius (with respect to the internal conductor) varies from 0 to 12 mm. The final extremity (antenna and end tip disc) is kept flush with the enlarged beam tube in any case. The coupling gain in the final design (Δr =8 mm) is 1.05 dB (+27 %) compared to an antenna without end disc (Δr =0). With this final geometry (fig.15 and 16) we get Qext=0.197×10^{6}: the goal coupling is overtaken by +0.67 dB.

As the curve is very flat for Δr between 6 and 10 mm, we expect this parameter (disc radius) not to be critical. As well, rounding the disc corners should have a negligible influence on the Qext.

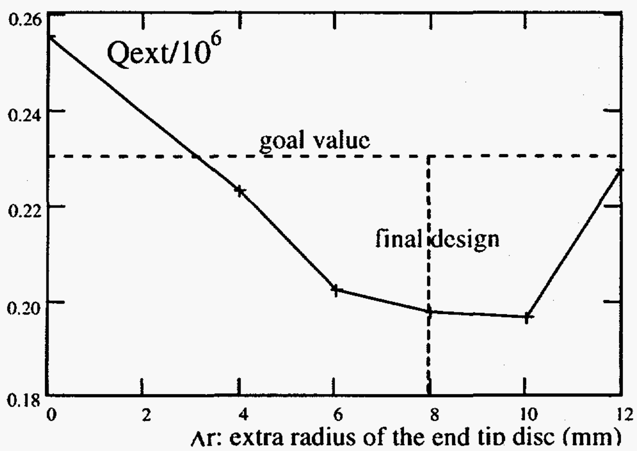

Fig. 14. Influence of end disc radius
in expanded beam-tube geometry.

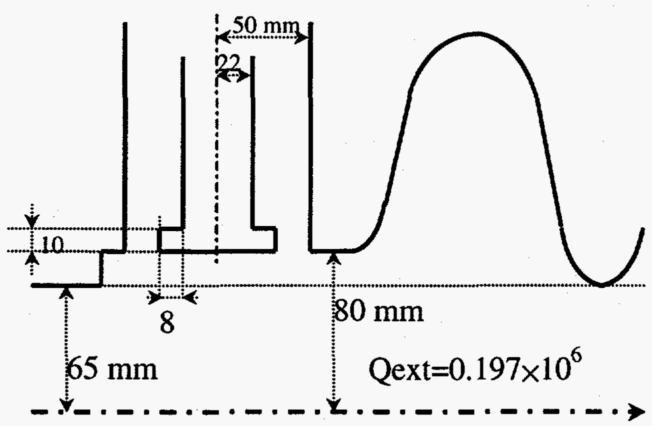

Fig. 15. Final geometry: the goal Qext is overtaken.

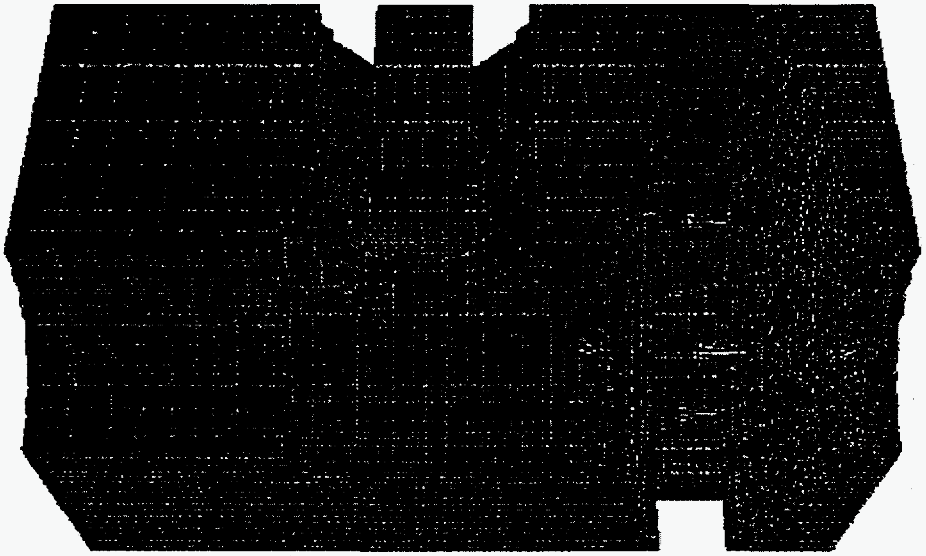

Fig 16. Final design geometry as computed by MAFIA.
The number of mesh points is about 155000.

6.3 Variations

For a final adjustment, couplers will be tuned by adjusting the penetration into the beam pipe. The Qext versus antenna penetration has been plotted on figure 17. Actually, in this simulation the end tip disc was a little smaller than in the final design (Δr=4mm instead of 8mm).

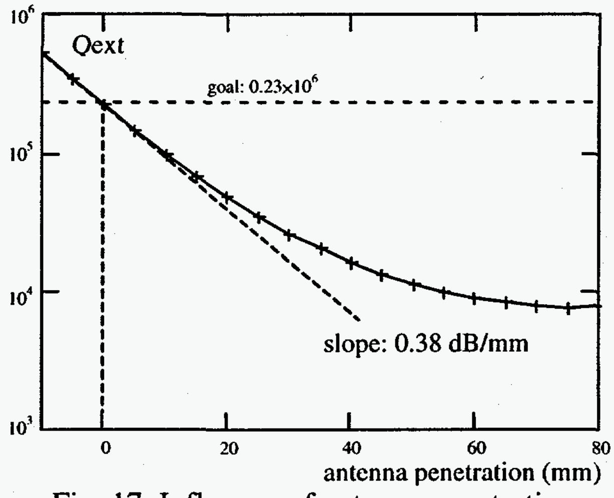

Fig. 17. Influence of antenna penetration
(computed with a Δr=4mm disc end-tip).

The influence of a possible antenna tilt was simulated by a parallel displacement of the antenna in the z-axis direction. The result is plotted on figure 18; the sign of the displacement is negative when directed toward the cells. The conclusion is that effect is very small: 0.12 dB/mm, i.e. 3.2 times less than antenna penetration. In other words, a ±1-mm misalignment can be compensated by a ±0.3-mm penetration of the antenna.

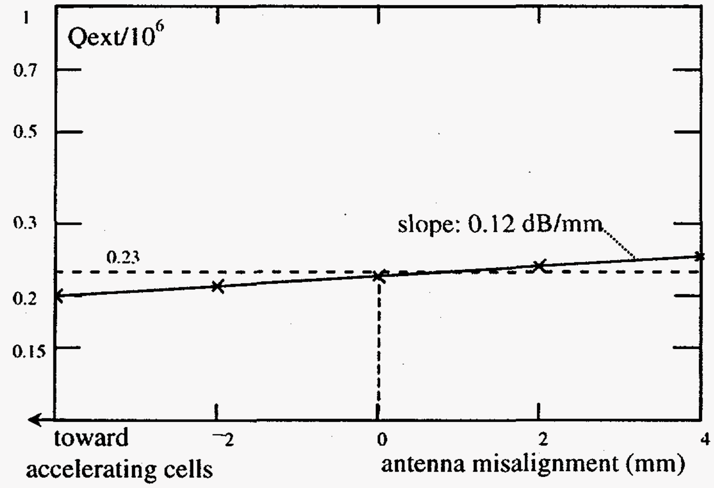

Figure 18. Qext versus antenna tilt.
(Computed with a Δr=4mm disc end-tip)

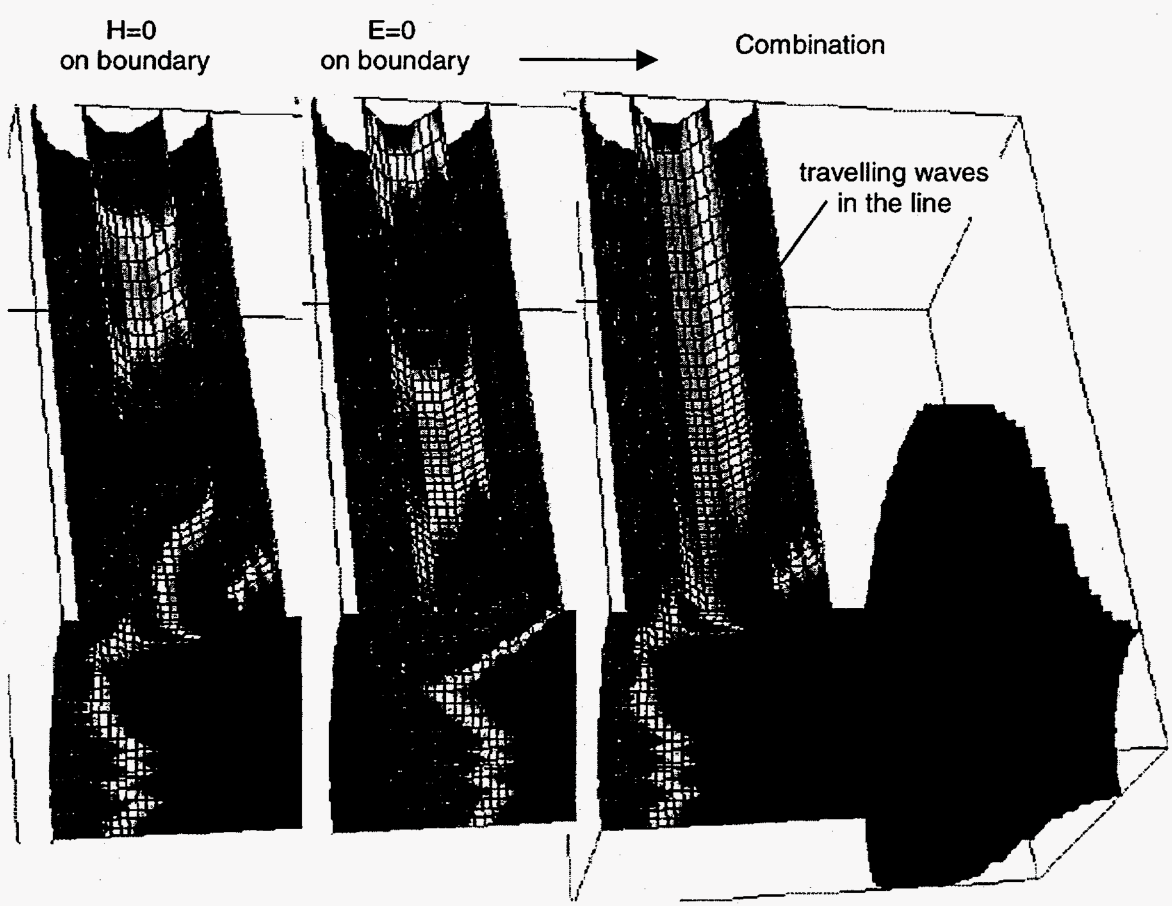

Fig. 19. Losses in the coupler under normal operations

6.4 Losses in an operating coupler.

According to the method described in section 2.4, the local losses in the coupler have been computed for the travelling wave. Again, the end tip disc was a little smaller than in the final design (Δr=4mm instead of 8mm). In figure 19, the losses of each of the two standing waves are displayed after normalization. After combination, the losses are uniform along the line (except in the end tip region). It proves that, as expected, the wave is a pure travelling one.

7. Qext computation for the β=0.82 cavity.

With the β=0.82 cavity characteristics, (E=5.5 MV/m, r/Q= 18.6, φ=29°), we get the required Qext: Qint=0.297×10^6. The cavity has been simulated with the same "final coupler geometry". The result is: Qext=0.328×10^6. We conclude that some modifications are also necessary for this cavity. Each of the solutions presented above for the β=0.64 cavity and its coupler may be considered to improve the coupling.

8. Conclusions

The Qext can be easily and efficiently computed by lossless cavity codes in frequency domain. The losses in the coupler associated with the travelling wave can also be derived from the same simulation.

The desired Qext in APT β=0.64 cavities has been obtained by expanding the beam-pipe. If necessary, an asymmetrical end tip and appropriate impedance steps could further improve the coupling.

With the present time design, the β=0.82 cavity is not sufficiently coupled. Either the cavity or its coupler should be modified.

Acknowledgements

The author is grateful to Frank Krawczyk for his help with MAFIA and for careful reading of the present paper. The author also thanks Henri Safa for his suggestions about the possible ways to improve the coupling.

References

[1] M. Prome, "Conceptual Studies for a High Power Proton Linac", LINAC-94, Tsukuba, p 146.

[2] F. Krawczyk et al., "The Power Coupler Design for the APT Superconducting Accelerator", LA-UR-97-3190, 8th Workshop on Superconducting RF, Abano Terme, Italy,1997.

[3] N.Kroll and D.Yu, "Computer determination of the external Q and resonant frequency of wave guide loaded cavities", Particle Accelerators, Vol 34, p 231, 1990.

[4] P.Balleyguier “A straightforward method for cavity external Q computation”, Particle Accelerators, Vol 57, p 113, 1997.

[5] W.Hartung and E.Haebel, “Search of trapped modes in the single-cell cavity prototype for CESR-B”, 1993 Particle Accelerator Conference, Washington DC, p 898.

[6] F. Krawczyk, et al, "Superconducting Cavities for the APT Accelerator", LA-UR-97-1700 and Proceedings of the 1997 PAC Conference in Vancouver, Canada.